Sex- and Isoform-Specific Mechanism of Neuroprotection by Transgenic Expression of P450 Epoxygenase in Vascular Endothelium

Jia Jia[e], **Catherine M Davis**[a], **Wenri Zhang**[a], **Matthew L. Edin**[b], **Sari Jouihan**[a], **Taiping Jia**[f], **J. Alyce Bradbury**[b], **Joan P. Graves**[b], **Laura M. DeGraff**[b], **Craig R. Lee**[c], **Oline Ronnekleiv**[f], **Ruikang Wang**[d], **Yun Xu**[g], **Darryl C. Zeldin**[b], and **Nabil J. Alkayed**[a]

[a]Department of Anesthesiology & Perioperative Medicine, The Knight Cardiovascular Institute, Oregon Health & Science University, Portland, OR, USA

[b]Division of Intramural Research, National Institute of Environmental Health Sciences, National Institutes of Health, Research Triangle Park, NC, USA

[c]Division of Pharmacotherapy and Experimental Therapeutics, Eshelman School of Pharmacy, University of North Carolina at Chapel Hill, Chapel Hill, NC, USA

[d]Department of Biomedical Engineering, University of Washington, Seattle, WA

[e]Jiangsu Key Laboratory of Translational Research and Therapy for Neuro-Psycho-Diseases and College of Pharmaceutical Sciences, Soochow University, Suzhou, Jiangsu, P.R. China

[f]Department of Physiology and Pharmacology, Oregon Health and Science University

[g]Department of Neurology, University of Nanjing School of Medicine, Nanjing, P.R. China

Abstract

Objective—Cytochrome P450 epoxygenases (CYP) metabolize arachidonic acid to epoxyeicosatrienoic acids (EETs), which exhibit vasodilatory, anti-inflammatory and neuroprotective actions in experimental cerebral ischemia. We evaluated the effect of endothelial-specific CYP overexpression on cerebral blood flow, inflammatory cytokine expression and tissue infarction after focal cerebral ischemia in transgenic mice.

Approach and Results—Male and female wild-type and transgenic mice overexpressing either human CYP2J2 or CYP2C8 epoxygenases in vascular endothelium under control of the Tie2 promoter (Tie2-CYP2J2 and Tie2-CYP2C8) were subjected to 60-minutes middle cerebral artery occlusion (MCAO). Microvascular cortical perfusion was monitored during vascular occlusion and reperfusion using laser-Doppler flowmetry and optical imaging. Infarct size and inflammatory

Corresponding author: Nabil J Alkayed, Anesthesiology and Perioperative Medicine, Knight Cardiovascular Institute, Oregon Health and Science University, 3181 SW Sam Jackson Park Road, Portland, Oregon 97239. alkayedn@ohsu.edu. 503-418-5502..

cytokines were measured at 24 hours of reperfusion by TTC and real-time quantitative PCR, respectively. Infarct size was significantly reduced in both Tie2-CYP2J2 and Tie2-CYP2C8 transgenic male mice compared to corresponding WT male mice (n=10 per group, p < 0.05). Tie2-CYP2J2, but not Tie2-CYP2C8 male mice maintained higher blood flow during MCAO; however, both Tie2-CYP2J2 and Tie2-CYP2C8 had lower inflammatory cytokine expression after ischemia compared to corresponding WT males (n=10 per group for CBF and n=3 for cytokines, p<0.05). In females, a reduction in infarct was observed in the caudate-putamen, but not in the cortex or hemisphere as a whole and no differences were observed in blood flow between female transgenic and WT mice (n=10 per group).

Conclusions—Overexpression of CYP epoxygenases in vascular endothelial cells protects against experimental cerebral ischemia in male mice. The mechanism of protection is in part linked to enhanced blood flow and suppression of inflammation, and is both sex- and CYP isoform-specific.

Keywords

stroke; eicosanoids; vasodilation; inflammation; cerebral blood flow

---

Introduction

Arachidonic acid (AA) is a polyunsaturated fatty acid present in cell membranes as part of their phospholipid pool (Liu et al., 2004). Free AA is released into cytosol upon stimulation by endogenous agonists, pharmacological agents and following injury, such as ischemic injury, where it is metabolized into biologically active eicosanoids by one of three enzymatic pathways: the cyclooxygenase (COX), lipoxygenase (LOX) or cytochrome P450 monooxygenase (CYP) pathway. There are two broad classes of CYP enzymes involved in eicosanoid formation: 1) the hydroxylases, which form 20-hydroxyeicosatetraenoic acid, a vasoconstrictor in the cerebral and coronary circulation; and 2) the epoxygenases, which form epoxyeicosatrienoic acids (EETs), which are vasodilators and protective against ischemic brain and heart injury by multiple mechanisms. In addition to vasodilation, EETs possess anti-inflammatory, anti-apoptotic and anti-oxidant properties (Spector and Norris, 2007). In the brain, EETs are produced by astrocytes (Alkayed et al., 1996), vascular endothelium (Medhora et al., 2001) and perivascular nerves (Iliff et al., 2007), where they have been implicated in functional hyperemia following neuronal activation (Alkayed et al., 1997, Harder et al., 1998). Interestingly, CYP epoxygenase upregulation in brain after ischemic preconditioning has been associated with tissue protection with no change in blood flow (Alkayed et al., 2002), suggesting that EETs may exert a neuroprotective effect that is independent from its established vasodilator effect. In contrast, stabilizing endogenous EETs by deleting their metabolizing enzyme soluble epoxide hydrolase (sEH) is protective against ischemic injury, and protection is clearly associated with increased vasodilation in response to focal cerebral ischemia (Zhang et al., 2008). Whether different regioisomers of EETs have different mechanisms of action and may account for these apparent differences following ischemia (neuroprotection versus vasodilation) is not well understood. Also, the contribution of EETs derived from different cell types to protection following ischemia has not been fully elucidated.

To determine the contribution of endothelial-derived EETs to protection following ischemia, we compared brain infarct and cerebral blood flow (CBF) during middle cerebral artery occlusion (MCAO) in transgenic mice overexpressing one of two human CYP epoxygenase isoforms, hCYP2J2 or hCYP2C8, in vascular endothelium. Our findings suggest that overexpression of CYP epoxygenase in vascular endothelium protects against experimental cerebral ischemia. The mechanism of protection is in part linked to enhanced blood flow and suppression of inflammation, and is both sex- and CYP isoform-specific.

Materials and Methods

The study was conducted in accordance with the National Institutes of Health guidelines for the care and use of animals in research, and protocols were approved by the Animal Care and Use Committee of Oregon Health and Science University (Portland, OR, USA).

Animals

Transgenic mice expressing either the human CYP2J2 or CYP2C8 epoxygenase in vascular endothelium under the control of the murine Tie2 promoter (2-kb) and full enhancer (10-kb) were generated on a C57Bl/6 background. We used heterozygous Tie2-CYP2J2, Tie2-CYP2C8 transgenic mice and age- and sex-matched WT littermate controls. Genotype was determined in each mouse by PCR of tail genomic DNA. Generation of Tie2-CYP2J2 and Tie2-CYP2C8 mice, founder lines, breeding and genotyping protocols have been previously described (Lee et al., 2010).

Middle Cerebral Artery Occlusion (MCAO)

Adult (25-28g) male and female wild-type (WT), Tie2-CYP2J2 and Tie2-CYP2C8 transgenic mice were subjected to 60-min middle cerebral artery occlusion (MCAO) under isoflurane anesthesia, as described previously, with slight modifications (Zhang et al., 2008). Briefly, mice were anesthetized with isoflurane (induction 5%; maintenance 1.0%), and kept warm with water pads. A small laser-Doppler probe was affixed to the skull to monitor cerebral cortical perfusion and verify vascular occlusion and reperfusion. A silicone-coated 6-0 nylon monofilament was inserted into the right internal carotid artery via the external carotid artery until laser-Doppler signal dropped to less than 20% of baseline. The animal was maintained anesthetized with 1% isoflurane on the surgical station for 60 minutes of occlusion. After reperfusion, mice were allowed to recover and observed for 24 hours. Infarct size was measured at 24 h after MCAO in 2-mm thick coronal brain sections (five total) using 2, 3, 5-triphenyltetrazolium chloride (TTC) staining and digital image analysis. Sections were incubated in 1.2% TTC in saline for 15 min at 37°C, and then fixed in formalin for 24 h. Slices were photographed; infarcted (unstained) and uninfarcted (red color) areas were measured with MCID software (InterFocus Imaging Ltd, Linton, UK) and integrated across all five slices. To account for the effect of edema, the infarcted area was estimated indirectly by subtracting the uninfarcted area in the ipsilateral hemisphere from the contralateral hemisphere, and expressing infarct volume as a percentage of the contralateral hemisphere. Cerebrocortical laser-Doppler perfusion (LDP) was monitored during occlusion and early reperfusion. The laser-Doppler probe was positioned on bone over the dorsolateral parietal cortex 2 mm posterior, 3 mm lateral to the Bregma. The LDP

signal was recorded continuously and averaged over 15-minute intervals for comparison among treatment groups.

Optical Microangiography (OMAG)

OMAG was performed as previously described (Zhang et al., 2009, An et al., 2010, Wang et al., 2007). The mouse head was shaved before OMAG imaging. During imaging, the mouse was immobilized on a custom-made stereotaxic stage and lightly anesthetized with isoflurane (0.2 l/min O2, 0.8 l/min air). Body temperature was kept at 35.5–36.5°C with a warming blanket and monitored by a rectal thermal probe throughout the experiment. An incision of ~1 cm was made along the sagittal suture, and the frontal parietal and interparietal bones were exposed by pulling the skin to the sides. The animal was then positioned under the OMAG scanning probe, allowing for visualization and quantification of blood flow based on endogenous light scattering from moving blood cells within biologic tissue, with no need to use exogenous contrasting agents. In the mouse, OMAG covers the entire thickness of the cerebral cortex through an intact skull. OMAG was an optical coherence tomography based imaging technique capable of generating three-dimensional images of functional vasculature in vivo and without the need for dye injection (An et al., 2010, Wang et al., 2007). The OMAG imaging system used in this study employed a superluminescent diode with a central wavelength of 1,310 nm and a full-width, half-maximum bandwidth of 50 nm, providing an axial resolution of ~10 um in tissue. The lateral resolution of the system was measured at ~15 um. The spectral interferograms formed by the reference light and the light backscattered from the tissue sample were detected by a custom-built, high-resolution and high-speed spectrometer, upon which the OMAG algorithm was applied to obtain angiographic images representing functional cerebral microvasculature within the scanned brain tissue. The three-dimensional scan represented a physical volume with the following x–y–z dimensions: $2.5 \times 2.5 \times 2.0$ mm3.

Isolation of Cerebral Vessels

Mice were deeply anesthetized with isoflurane and perfused transcardially with pre-chilled heparinized saline (1 U/ml) before decapitation to remove blood from the cerebral circulation; brains were then rapidly dissected. Pial and large cerebral vessels were removed with fine forceps and discarded. The remaining brain tissue was homogenized in ice-cold PBS with a loosely fitting Dounce homogenizer, and centrifuged at 2,000 g for 5 minutes at 4°C. The supernatant, containing parenchymal brain tissue, was discarded; the pellet, containing vessels, was resuspended in PBS and centrifuged at 2,000 g for another 5 minutes at 4°C. The second pellet was resuspended in PBS, layered over a 15% dextran density gradient (molecular weight 35,000 - 40,000 kDa), and centrifuged in a swinging-bucket rotor for 30 minutes at 3,500 g at 4°C. The supernatant was discarded, and the pellet was resuspended in PBS, and again layered over dextran and centrifuged for an additional 30 minutes at 3,500 g. The resulting pellet was washed with ice-cold PBS over a 70 mm nylon mesh, cerebral microvessels vessels and capillaries were collected and stored at −80 °C.

Primary aortic endothelial cell isolation

Aorta from WT Tie2-CYP2J2 and Tie2-CYP2C8 male mice were harvested for isolation of endothelial cells, as described previously (Lee et al., 2010). Briefly, 3 aortas from each

genotype were pooled, minced and digested with type-I collagenase (2 mg/ml, Worthington Biochemical Corporation, Lakewood, NJ, USA) at 37°C for 45 min. Resultant homogenates were triturated with a 30-ml syringe, filtered through a 70-μm cell strainer, washed with PBS + 0.1% FBS and centrifuged for 10 minutes at 1000rpm. Cell pellets were re-suspended and incubated with magnetic Dynabeads (Invitrogen) coated with anti-CD31 antibody (BD Biosciences, San Jose, CA, USA). Endothelial cells were isolated by magnetic separation and plated onto 0.1% gelatin-coated flasks in DMEM supplemented with 20% FBS, 100 μg/mL heparin, 100 μg/mL penicillin/streptomycin and 100 μg/mL endothelial cell growth supplement (Biomedical Technologies, Stoughton, MA, USA). Once confluent, cells were trypsinized and further purified by incubation with anti-CD102 (BD Biosciences) coated Dynabeads and grown to confluence. 1 million endothelial cells were plated on 100 mm tissue culture dishes and allowed to adhere overnight. Cells were washed with PBS and incubated in serum free DMEM for 4 hours. The cell- conditioned medium was collected, the cells were then incubated for 10 minutes in fresh serum free DMEM containing 10 μM Ca^{2+} ionophore (A23187, Sigma-Aldrich) to stimulate arachidonic acid release. Both basal and stimulated medium were collected and stored at −80°C for MC/MS/MS analysis.

Quantification of CYP-derived eicosanoids in medium

Epoxy and dihydroxy metabolites (EETs and DHETs) of arachidonic acid were extracted and quantified; 11,12- and 14,15- regioisomers specifically were quantified as these are the primary metabolic products synthesized by CYP2J2 and CYP2C8 (Zeldin et al., 1995; Wu et al., 1996). These were extracted in cell culture medium by solid-phase extraction and eluted in ethyl acetate, as described by Newman et al. (2002) and Seubert et al. (2006). Oxylipids were separated by reverse-phase HPLC on a 2- × 150-mm, 5-μm Luna C18 (2) column (Phenomenex, Torrance, CA, USA) and quantified using a MDS Sciex API 3000 triple quadrupole mass spectrometer (Applied Biosystems) with negative mode electrospray ionization and multiple reaction monitoring, as previously described (Newman et al., 2002). Relative response ratios of each analyte were used to calculate concentrations, quantification relative to internal standards corrected for surrogate losses. Cell medium concentrations were normalized to cell plating density.

Cerebrospinal fluid (CSF) collection and extraction

Plasma oxylipid levels were determined by liquid chromatography, tandem mass spectroscopy (LC/MS/MS). Samples were collected from the cisterna magna of naïve animals. Mice were anesthetized and placed prone on a stereotaxic frame. A sagittal incision of the skin was made inferior to the occiput, the subcutaneous tissue and muscles separated and the dura matter was penetrated with the 30G1 needle connected with PE-10 tube. The CSF was drawn into PE-10 tubing with the careful suction by a 10 μl gastight syringe (Hamilton Company, Reno, NV, USA). The CSF was injected into an Eppendorf tube, and frozen in a −80°C freezer until assayed. CSF samples (5-10 ul) were mixed with 50 ul of 0.1% acetic acid in 5% methanol, 10 ul of 0.4mg/ml butylated hydroxytolulene, and spiked with with 30 ng PGE2-d4, 10,11- DiHN, and 10,11-EpHep (Cayman Chemical, Ann Arbor, MI) as internal standards. Oxylipids were extracted 3 times with 1 ml ethyl acetate. Ethyl acetate from each sample was pooled and dried under gentle nitrogen flow. Samples were reconstituted in 100 ul of 40% ethanol. Three injections of 20 ul were analyzed for each

sample. The triplicate sample injections were averaged, corrected for volume of CSF, and represented as pg/ul. Online liquid chromatography of extracted samples was performed with an Agilent 1200 Series capillary HPLC (Agilent Technologies, Santa Clara, CA, USA) as previously described (Edin et al., 2011, Newman et al., 2002). Separations were achieved using a Phenomenex Luna C18(2) column (5 um, 150×1 mm; Phenomenex, Torrance, CA, USA), which was held at 40°C. Mobile phase A was 85:15:0.1 water:acetonitrile:acetic acid. Mobile phase B was 70:30:0.1 acetonitrile:methanol:acetic acid. Gradient elution was used; mobile phase percentage B and flow rate were varied as follows: 0% B at 87.5 ul/min at 0 min, ramp from 0 to 2 min to 25% B at 87.5 ul/min, ramp from 2 to 5 min to 50% B at 60 ul/min, ramp from 5 to 23 min to 92.5% B at 60 ul/min, ramp from 23 to 23.5 min to 100% B at 87.5 ul/min, hold from 23.5 to 29 min at 100% B, ramp from 29 to 29.6 min down to 0% B, and hold 0% B to 33 min. Negative ion electrospray ionization tandem mass spectrometry was used for detection. Analyses were performed on an MDS Sciex API 3000 equipped with a TurboIonSpray source (Applied Biosystems). Turbo desolvation gas was heated to 275°C at a flow rate of 5.75 ml/min.

TaqMan Real-Time Quantitative PCR

RNA was isolated from cerebral microvessels using RNAqueous-Micro kit and reverse transcribed using the High Capacity cDNA Reverse Transcription Kit; resultant cDNA was amplified using TaqMan Universal PCR Master Mix (all Life Technologies, Carlsbad, CA) in the ABI Prism 7000 sequence detection system. Quantitative PCR was performed in 96 well plate format using 50 μl total volume, with each sample run in triplicate. PCR was also run on controls in which template had not been added, in order to determine DNA contamination and primerdimer formation. RNA with no reverse transcription was also included to discount genomic DNA amplification. TNFα (Mm00443258_m1) and IL1-β (Mm00434228_m1) gene expression assays (Life Technologies) were used and 18S was measured as an internal control using the 18S rRNA control kit FAM-TAMRA (Eurogentec SA, Osaka, Japan). Relative quantification analysis was performed using the 2(−Delta Delta C(T)) method (Livak et al., 2001).

In situ hybridization

Cloning of human CYP 2C8 and 2J2—Fragments of the human CYP 2C8 and 2J2 gene were cloned by using TOPO TA Cloning kit (Thermo Fisher Scientific, Waltham, MA). The forward primer (bases 869-888; 5'-CAA TCC TCG GGA CTT TAT CG-3') and reverse primer (bases 1182-1163; 5'-GGA CAA GGT CAC TGT ATC TC-3') for 2C8 were designed from the human 2C8 sequence (accession number NM_000770). The forward primer (bases 942-961; 5' ACC GAG ACA ACT TGG ACA AC-3') and reverse primer (bases 1347-1328; 5'-ATG CCC GCT TTC CTA TTG AG-3') for 2J2 were designed from the human 2J2 sequence (accession number NM_000775). The CYP 2C8 and 2J2 fragments were amplified from aMHC-2C8 and aMHC-2J2 constructs. PCR was conducted for 40 cycles of denaturation (95°C, 45 seconds), annealing (61.6°C, 45 seconds), and extension (72°C, 1 minute). The resulting 314bp (2C8) and 406bp (2J2) products were subcloned into the pCR2.1-TOPO vector (Invitrogen) using the TOPO TA cloning kit according to the manufacturer's instruction. The pCR2.1-TOPO vector contains only one promoter (T7), therefore, sense and antisense probes required two separate vectors with the respective

inserts in the correct orientation for sense and antisense synthesis. The vectors containing the inserts were then sequenced to confirm the direction for sense and antisense probe synthesis.

Probe preparation—Radioactive antisense and sense cRNA probes were transcribed in vitro with T7 RNA polymerase from the BamH1 linearized human CYP 2C8 and 2J2 constructs in the presence of 35S-uridine 5' (α-thio)triphosphate (35S-UTP). Residual DNA was digested with 2 U DNase I (Ambion Inc. Austin, Texas). The sense and antisense RNA probes were purified on a G-50 Sephadex column (Amersham Biosciences, Piscataway, NJ).

Tissue preparation—Wild-type and transgenic animals were anesthetized, killed by decapitation and the brains sliced into 2 mm coronal blocks through the rostral forebrain. The brain blocks were fixed by immersion in 4% paraformaldehyde in Sorensen buffer (0.03 M; pH 7.4) for 6 hours at 4°C, rinsed overnight in 20% buffered-sucrose solution (pH 7.4), embedded in O.C.T. (Sakura Finetek, Torrance, CA), and frozen in isopentane at −55°C. Coronal sections (20 μm) were cut on a cryostat and thaw mounted onto Superfrost Plus glass slides (Thermo Fisher Scientific). The sections were stored at −80°C.

Hybridization—The slides were postfixed in fresh 4% paraformaldehyde in Sorensen's phosphate buffer (0.03 M, pH 7.4) for 20 minutes, rinsed with Sorenson's phosphate buffer, and treated with proteinase K (1.0 μg/ml) for 4 minutes at room temperature. Sections were then treated with 0.1 M triethanolamine (3 minutes), followed by 0.25% acetic anhydride in 0.1 M triethanolamine (10minutes) (Sigma- Aldrich, St Louis, MO). Sections were prehybridized for 1 hour at 58°C with hybridization buffer (50% formamide, 1x Denhardt's solution, 10% dextran sulfate, 100 μM dithiothreitol [DTT], 200 mM sodium chloride, 10 mM Tris-HCl, pH 8.0, 1 mM EDTA, pH 8.0, 125 μg/ml tRNA; Sigma- Aldrich) and then quickly rinsed in 2xSSC buffer. The 35S-labeled antisense as well as sense riboprobes were heat-denatured, diluted with hybridization buffer, and used at a final concentration of 2×10^4 cpm/μl. Subsequently, the sections were covered with glass coverslips, sealed, and hybridized in a moist chamber for at least 18 hours at 58°C. After hybridization, the slides were washed in 2x SSC buffer at 62°C four time with three changes, reacted with RNAse (20 μg/ml) for 30 minutes at 37°C, and washed in decreasing concentrations of SSC (2x, 1x, 0.5x, 0.25x) at 58°C for 10 minutes each with three changes of each solution. Finally, the slides were washed in 0.1x SSC with 1mM DTT for 45 minutes at 58°C. The slides were dehydrated in 50%, 80% and 90% ethanol with 300mM Ammonium Acetate followed by 100% ethanol for 2 minutes, placed side by side on a flat surface together with autoradiographic 14C microscales, and exposed to Hyperfilm-βmax (Amersham Biosciences, Piscataway, NJ) for 6 days at 4°C. The films were developed in D19 developer for 5 minutes, fixed in Kodak fixer for 5 minutes. The slides were then dipped in Kodak NTB-2 nuclear track emulsion and exposed for 21 days at 4°C. Thereafter, slides were developed in D19 developer for 2 minutes, fixed in Kodak fixer for 5 minutes, counterstained with hematoxylin, dehydrated, and coverslipped.

Film images were scanned (HP Scanjet 7400c) and digitized images processed in Adobe Photoshop (Mountain View, CA) and Macromedia FreeHand (San Francisco, CA). Contrast and brightness were adjusted in scanned images of films to compensate for uneven

illumination in brightfield images. Images of emulsion-coated slides were analyzed using a Nikon E800 microscope. Darkfield and brightfield images were captured using a Nikon DS-L1 digital camera and illustrated in Adobe Photoshop and Macromedia FreeHand software programs. Contrast and brightness were adjusted in scanned images to match the original image seen in the microscope.

Statistical Analysis

Data were expressed as mean ± SEM. Infarct size, LDP bar graph and LC/MS/MS data were analyzed with one- or two- way analysis of variance (ANOVA), as appropriate, and post hoc Dunnett's multiple comparisons test using GraphPad Prism Software (version 3.1, SPSS Inc., La Jolla, CA, USA). Laser Doppler perfusion data were analyzed with two-way repeated measure ANOVA with Tukey's multiple comparisons test, while qPCR data were analyzed with two-way ANOVA with Tukey's multiple comparisons test. $p < 0.05$ was considered statistically significant.

Results

Expression and distribution of human CYP2J2 and CYP2C8 transgenes in mouse brain

In situ hybridization was used to determine endothelial expression of human CYP2J2 and CYP2C8 in brains of Tie2-CYP2J2 and Tie2-CYP2C8 female mice, respectively (Figure 1). [^{35}S]-labeled antisense and sense cRNA probes prepared from the respective human sequences were used. Antisense probes produced hybridization signal in transgenic but not in WT littermate brain, and sense probes did not generate signal in transgenic brains (WT and sense hybridization not shown), indicating specificity of probe for the human transgenes. Localization of CYP2J2 and CYP2C8 transgenes broadly follow the vascular distribution in brain, as shown in representative sections from rostral to caudal forebrain in Figure 1A (a-c for CYP2J2, d-f for CYP2C8). It is of note that CYP2J2 mRNA is also expressed in ependymal cells lining the lateral or third ventricle in contrast to CYP2C8 mRNA expression, which was limited to pial and parenchymal vessels. This can be clearly seen by comparing panels labeled c1 and c2 in Figure 1B and 1C. Higher magnification images are shown in 1B (CYP2J2) and 1C (CYP2C8), from top to bottom, of coronal sections through the rostrodorsal cortex (region labeled CTX in 1A), lateral ventricular area (LV) and olfactory cortex (CYP2J2)/ optic chiasm (CYP2C8), demonstrating vascular expression pattern for both transgenes. Another difference observed in expression between transgenes is the abundant expression of CYP2C8 in the choroid plexus, which is absent for CYP2J2 (not shown).

Transgenic expression of CYP2J2 and CYP2C8 in endothelium is protective against experimental stroke

To determine if endothelial expression of CYP2J2 or CYP2C8 epoxygenase alters outcome from experimental stroke, we compared cortical and striatal (caudate-putamen, CP) infarcts in Tie2-CYP2J2 and Tie2-CYP2C8 mice to those in WT, both in male and female mice. In males, both cortical and striatal infarcts were significantly smaller in transgenic mice compared to WT littermates (Figure 2A), with cortical infarct decreasing from 45.01 ± 3.1% of contralateral structure in WT to 25.75 ± 5.3% in Tie2-CYP2J2 and 22.10 ± 4.7% in Tie2-

CYP2C8 mice. In females, striatal infarct was reduced from $70.36 \pm 5.4\%$ of contralateral structure in WT to $55.24 \pm 5.2\%$ in Tie2-CYP2J2 and $55.43 \pm 7.1\%$ in Tie2-CYP2C8 (Figure 2B). However no reduction in infarct was observed in either the cortex or the hemisphere as a whole.

No differences were observed in body weight, anesthesia requirement or body temperature between WT and transgenic mice.

Transgenic expression of CYP2J2 in endothelium increases collateral blood flow in male mice

To determine if the decrease in infarct size in Tie2-CYP2J2 and Tie2-CYP2C8 transgenic mice was linked to increased CBF, we compared laser-Doppler cortical perfusion (LDP) during MCAO between WT and transgenic mice. Figure 3A shows that in males, LDP during MCAO was significantly higher in Tie2-CYP2J2 ($19.76 \pm 0.80\%$ relative to baseline), but not in Tie2-CYP2C8 ($15.29 \pm 0.73\%$), compared to WT mice ($12.09 \pm 0.23\%$). In females, there were no differences in LDP during ischemia between WT ($12.51 \pm 0.35\%$) and either of the two transgenic mouse lines (Figure 3B). Following 5 minutes of reperfusion, LDP in males was significantly higher in Tie2-CYP2J2 ($115.8 \pm 6.8\%$) and Tie2-CYP2C8 ($107.9 \pm 5.7\%$) compared to WT ($88.33 \pm 6.1\%$). In females, LDP after 5 minutes of reperfusion was also elevated in Tie2-CYP2C8 mice (120 ± 10.6) compared to both WT (98.17 ± 6.0) and Tie2-CYP2J2 mice ($99.22 \pm 5.9\%$).

We further carried out non-invasive optical microangiography (OMAG) in male WT and Tie2-CYP2J2 mice. We chose to evaluate microvascular perfusion in the CYP2J2 males as this was the only group to display increased LDP during the time of occlusion (Figure 3A). We found that despite filament withdrawal and reperfusion through proximal MCA branches (as indicated by the return in LDP to baseline in Fig 3A), distal microvascular perfusion was still impaired in the WT ischemic hemisphere (I) at 24 hours after MCAO (compared to contralateral hemisphere, Figure 3C). Importantly, male Tie2-CYP2J2 mice, as well as demonstrating higher LDP during time of occlusion, were also protected from delayed post-ischemic microvascular hypoperfusion.

To determine whether the protection enjoyed by male mice with transgenic expression of CYP2J2 and CYP2C8 in endothelium was in fact due to increased CYP activity, rather than an off target effect of the transgene, infarct size and cortical perfusion after MCAO were measured in the presence of CYP inhibitor, MS-PPOH (Figure 4). Male mice were used since they displayed a more robust protection from MCAO than females (Figure 2). Mice were implanted with an osmotic pump containing 2.5 mg / ml MS-PPOH or vehicle (ethanol) prior to MCAO and kept for 24 hours after MCAO. Inhibition of CYP epoxygenase activity abolished the protective effect of the transgenes in male mice, as infarct size after MCAO was no longer different in Tie2-CYP2J2 or Tie2-CYP2C8 male mice compared to WT male mice (Figure 4A). Similarly, no differences were observed in LDP during MCAO between transgenic and WT mice (Figure 4B).

Attenuation of post-ischemic inflammatory response in male mice with endothelial expression of CYP2J2 and CYP2C8

Because male Tie2-CYP2C8 mice were protected from ischemic injury compared to WT control mice, yet there were no differences in cortical perfusion during occlusion between the two groups, we investigated a possible anti-inflammatory mechanism of protection by CYP2C8. Using rt-qPCR, we measured pro-inflammatory cytokine expression in microvessels isolated from ischemic and contralateral hemispheres, as well as from naïve brains of male WT, Tie2-CYP2J2 and Tie2-CYP2C8 mice. We found that in WT mice, mRNA levels of both TNFα (Figure 5A) and IL1-β (Figure 5B) are significantly increased in microvessels from the ipsilateral hemisphere 24 hours following MCAO, compared to microvessels extracted from naïve brains. There was also a slight increase in contralateral hemisphere after MCAO (over levels in naive brain), but the increase was not statistically significant. Endothelial expression of CYP epoxygenase prevented pro-inflammatory cytokine expression after ischemia, as transgenic Tie2-CYP2J2 and Tie2-CYP2C8 mice did not show an increase in expression after MCAO.

Increase in fatty acid metabolites in Tie2-CYP2C8 male mice

Since CYP 450 epoxygenases metabolize AA to form EETs, we investigated the effect of endothelial expression of these two CYP isoforms on release of 11,12- and 14,15- EETs, also assessing their stable metabolites, 11-12- and 14,15- DHETs; these regioisomers were investigated since these are the primary metabolic products synthesized by CYP2J2 and CYP2C8 (Wu et al., 1996; Zeldin et al., 1995). Primary aortic endothelial cells from WT, Tie2-CYP2J2 and Tie2-CYP2C8 male mice were isolated and cultured and the release of EETs and DHETs into the culture medium by these cells was measured, both in the quiescent state and also following stimulation with 10 μM A23187 calcium ionophore for 10 minutes which acts to liberate arachidonic acid from the plasma membrane. Our results show that, in the quiescent, unstimulated state, endothelial cells isolated from Tie2-CYP2J2 mice release significantly higher concentrations of 11,12- EET and DHET into the medium compared to cells isolated from WT mice (14.05 ± 1.0 and 8.83 ± 0.8 pg/ million cells respectively for 11,12- EET and DHET combined). However, cells stimulated with A23187 show a different response, in this paradigm cells isolated from Tie2-CYP2C8 mice release higher concentrations of 11,12-, and 14,15- EET and DHET combined compared to WT (27.14 ± 1.7 vs. 20.68 ± 2.0 and 65.76 ± 3.3 vs. 42.79 ± 5.4 pg/ million cells respectively), while cells isolated from both Tie2-CYP2J2 and Tie2-CYP2C8 transgenic lines release more 14,15- EET than WT cells (18.44 ± 0.9 and 19.38 ± 0.6 compared to 12.96 ± 0.5 pg/million cells respectively). No difference was observed in levels of 11,12- EET itself following A23187 stimulation in endothelial cells derived from either transgenic line.

We also investigated the effect of endothelial expression of these two CYP isoforms on levels of fatty acid metabolites in cerebrospinal fluid (CSF) of male WT, Tie2-CYP2J2 and Tie2-CYP2J2 mice using liquid chromatography-tandem mass spectrometry (LC-MS/MS). We first measured levels of AA metabolites (Figure 7A). Although CSF levels of EETs were below detection, we were able to measure their stable metabolites, DHETs. Levels of both 11,12- and 14,15-DHET were significantly increased in Tie2-CYP2C8 mice (0.21 ± 0.03 and 0.33 ± 0.05 pg/ μl respectively) compared to WT (0.10 ± 0.02 and 0.18 ± 0.02 pg/ μl

respectively), while no increase was observed in mice expressing CYP2J2. CYP2C8-, but not CYP2J2-expressing mice also displayed increased levels of the LOX metabolite of AA, 12-HETE, while levels of 5- and 15-HETE remained unchanged compared to WT. CSF levels of COX metabolites of AA, 6-keto-prostaglandin (6-keto-PGF$_{1\alpha}$), thromboxane B2 (TXB$_2$), prostaglandin F2α (PGF$_{2\alpha}$) and prostaglandin E2 (PGE$_2$), were not different from WT in either of the transgenic strains. We also measured CYP products of linoleic acid and DHA metabolism (Figure 7B). Levels of the linoleic acid epoxides, 12,13- and 9,10- epoxy-octadecamonoenoic acid (EpOME), were below the level of detection. We were able to quantify dihydroxy-octadecamonoenoic acid (12,13-DiHOME); however no difference among genotypes was observed. The epoxide product of docosahexaenoic acid (DHA) metabolism by CYP, 19,20-epoxydocosapentaenoic acid (19,20-EpDPE), showed no difference in CSF levels among genotypes; however, its metabolic product 19,20-dihydroxydocosapentaenoic acid (19,20-DiHDPA) was increased in Tie2-CYP2C8 mice compared to WT control CSF (0.49 ± 0.06 to 1.33 ± 0.27 pg/ μl respectively).

Discussion

The main findings of our study are: 1) transgenic expression of CYP epoxygenase in vascular endothelium reduces infarct size after MCAO in male and female mice, decreasing infarct in the hemisphere as a whole in males but not females; 2) transgenic endothelial expression of CYP2J2, but not CYP2C8 enhances blood flow during MCAO in male, but not female mice, and improvement in microvascular perfusion is maintained during reperfusion; 3) in males transgenic endothelial expression of either CYP2J2 or CYP2C8 attenuates post-ischemic expression of pro-inflammatory cytokines in cerebral microvessels; 4) male Tie2-CYP2J2 endothelial cells produce increased 11,12-EET in the quiescent state; 5) upon liberation of AA from the plasma membrane endothelial cells from both transgenic lines produce increased 14,15-EET, while Tie2-CYP2C8 also produce increased levels of 11,12 EET and DHET, and 6) male Tie2-CYP2C8 mice have higher CSF levels of CYP metabolites of AA and DHA.

The biological activity of EETs is terminated through multiple pathways (Zeldin, 2001), including metabolism by soluble epoxide hydrolase (sEH) into less active vicinal diols referred to as dihydroxyeicosatrienoic acids (DHETs). We have previously demonstrated that mice with sEH gene deletion (sEH knockout, sEHKO) have higher circulating 14,15-EET and enhanced collateral perfusion in response to focal vascular occlusion, resulting in reduced ischemic brain tissue damage (Zhang et al., 2008). These findings suggested that increasing EETs bioavailability by decreasing their metabolism may protect against stroke. Indeed, pharmacological inhibition of sEH was shown to reduce infarct size after MCAO in mice and to attenuate neuronal cell death in culture induced by oxygen-glucose deprivation (OGD) (Koerner et al., 2007, Zhang et al., 2007). Since sEHKO mice have global deletion of sEH, resulting in increased EETs in all cell types, we wondered about the specific contribution of endothelial EETs to protection from cerebral ischemia. In the current study we therefore examined the effect of transgenic overexpression of two cytochrome P450 epoxygenase isoforms in vascular endothelium under control of the Tie2 promoter (Schlaeger et al., 1997) on blood flow and infarct size after MCAO in male and female mice. We examined males and females separately because of previous reports demonstrating sex

differences in P450 epoxygenase expression (Athirakul et al., 2008). We focused on CYP2C8 and CYP2J2 isoforms because these two human isoforms are highly expressed and major contributors to EETs biosynthesis in myocardial and vascular tissue (Enayetallah et al., 2004, Larsen et al., 2006). However, their contribution to the pathogenesis of cerebrovascular disease has not been well characterized to date.

Our data suggest that male mice are protected from ischemic injury by overexpression of CYP epoxygenase in vascular endothelium, regardless of whether the specific isoform is CYP2J2 or CYP2C8. The protection by CYP2J2, but not CYP2C8 overexpression was associated with increased blood flow during MCAO. Interestingly, Tie2-CYP2J2 mice also had improved microvascular perfusion at 24 hours after MCAO. Microvascular hypoperfusion at this point occurs as a result of multiple pathological mechanisms, including vasoconstriction, microthrombosis, inflammation, and endothelial injury and swelling. Our observation that CYP2J2 protects against this injury suggests that EETs either protect endothelial cells against the initial endothelial oxidative injury during ischemia-reperfusion or blocks downstream inflammatory and pro-thrombotic mechanisms.

Because infarct size was smaller in Tie2-CYP2C8, though unlike Tie2-CYP2J2, collateral blood flow was not increased, we searched for a non-vascular mechanism of protection by endothelial expression of CYP2C8. Since EETs possess anti-inflammatory properties in the vasculature (Node et al., 1999), and ischemia-induced expression of inflammatory cytokines in brain is attenuated in sEH knock-out mice (Koerner et al., 2008), we tested the hypothesis that transgenic endothelial expression CYP2C8 would attenuate MCAO-induced upregulation of cytokine mRNA expression in cerebral microvessels. We found that endothelial overexpression of either isoform prevented ischemia-induced cytokine expression that is observed in WT microvessels after MCAO. Our observation supports recent studies demonstrating anti-inflammatory roles for CYP2J2 both in cultured pulmonary endothelial cells and following ischemia/ reperfusion injury in the lung (Feng et al., 2013, Chen et al., 2015), and CYP2C8 in cultured human umbilical vein endothelial cells (Liu et al., 2014).

Following stimulation of aortic endothelial cells isolated from these mice with a calcium ionomophore to induce AA release from the plasma membrane, a phenomenon which also occurs following ischemic insult, we see an increase in the production of EETs and their DHET metabolites by both CYP isoforms. It is interesting to note that despite Tie2-CYP2J2 demonstrating both increased blood flow and decreased inflammatory cytokines, endothelial cells from these mice produce increased 14,15- EET following A23187 stimulation, but no increase in 11,12- EET. However the Tie2-CYP2C8 mice which were also protected from injury and had a reduction in inflammatory cytokines with no increase in blood flow during occlusion, showed increases in both 11,12- EET metabolites and 14,15- EET.

We also measured CSF levels of fatty acid metabolites in CSF collected from male mice. We found increased level of 11,12- and 14,15-DHET in Tie2-CYP2C8, likely reflecting increased synthesis of 11,12- and 14,15-EET, the two main metabolites produced by CYP2C8 (Daikh et al., 1994). Surprisingly we did not observe increased CSF DHETs in Tie2-CYP2J2, although we did observe increased EET/ DHET release by endothelial cells

from these mice. The lack of increased DHET in CSF may reflect limited substrate (AA) availability, especially since these were naïve mice and AA liberation from the plasma membrane occurs following injury or other stimulation. We also observed increased 19,20-DiHDPA in CSF from Tie2-CYP2C8 mice, likely reflecting increased formation of 19,20-EpDPE by CYP2C8 from DHA (Zhang et al., 2014), an essential fatty acid and the most abundant ω-3 fatty acid in neural tissues. A similar increase in plasma 19,20-EpDPE was also previously observed in Tie2-CYP2C8 (Shao et al., 2014). Finally, Tie2-CYP2C8 CSF also had increased levels of 12-HETE; although 12/15-HETEs are primarily produced via the lipoxygenase pathway, they have also been reported to be produced by members of the 2C epoxygenase family, including CYP2C8 (Rifkind et al., 1995, Bylund et al., 1998).

In contrast to males, transgenic expression of CYP2J2 or CYP2C8 in endothelium did not alter CBF during MCAO in females and reduced infarct only in the striatum, though had no effect on the brain hemisphere as a whole. This observation suggests that the P450 epoxygenase pathway plays a differential role in ischemic neuroprotection between males than females. Consistent with this concept, dilations to endothelium-derived hyperpolarizing factor (EDHF) in rat middle cerebral artery (MCA) are less pronounced in females compared to males (Golding et al., 2001). In coronary, cerebral, renal, and skeletal muscle circulations, EDHF has been suggested to be a cytochrome P450 epoxygenase metabolite (Alkayed et al., 1996, Fisslthaler et al., 1999, Fulton et al., 1992, Huang et al., 2000, Davis et al., 2011). The absence of protection in females by transgenic CYP expression in endothelium suggests that females use a different mechanism for blood flow regulation in the ischemic brain. One such mechanism could be endothelial nitric oxide (eNOS), which is enhanced by chronic estrogen treatment (Athirakul et al., 2008, Goetz et al., 1994). For example, substance P- and shear stress-induced dilation of skeletal muscle arterioles was greater in female than male rats, linked to greater release of NO in females (Huang and Kaley, 2004, Huang et al., 1998, Huang et al., 1997). However, when eNOS is absent, as in the case of eNOS knockout mice, females use the P450 epoxygenase pathway to mediate flow-induced dilation in skeletal muscle arterioles (Huang et al., 2000).

Alternatively, it is perhaps not surprising that transgenic expression of the CYP isoforms did not protect female mice from ischemic damage. Female WT mice sustain smaller infarcts than males following MCAO while also maintaining higher CBF during occlusion. They also have lower sEH levels in the brain and higher circulating EETs than males. We have previously demonstrated that the sex difference in infarct size is abolished in global sEH knock-out mice, where male infarct size is reduced to that observed in females (Zhang et al., 2014). Overexpression of CYP enzymes in one cell type in the brain may therefore not afford additional benefit to females who already benefit from higher levels of EETs. Whereas males, who have lower EETs, would benefit from increased generation of EETs by the endothelium. Although we did not carry out a side-by-side comparison of expression levels of the transgenes between males and females, we do demonstrate robust expression of both transgenes in the female brain by in situ hybridization. Therefore the lack of protection from ischemic insult in female WT vs. Tie2 mice does not appear to be due to a lack of expression of the Tie2- driven CYP enzymes.

In summary, the current study examined the effects of transgenic expression of cytochrome P450 epoxygenase in vascular endothelium on focal cerebral ischemic injury in mice. We demonstrate that endothelial overexpression of two distinct human CYP isoforms is protective in male mice. The mechanism of protection is dependent on which CYP isoform is expressed, which is likely mediated by suppression of ischemia-induced inflammation in Tie2-CYP2C8 mice, and a combination of anti-inflammatory mechanism with enhanced blood flow in Tie2-CYP2J2 mice. In contrast, transgenic expression of CYP epoxygenase in females did not alter blood flow or hemispheric infarct size after MCAO. These findings suggest that the efficacy and mechanism of protection of any therapeutic strategies targeting the cytochrome P450 epoxygenase pathway may be influenced by sex and the specific CYP isoform involved.

Acknowledgments

Abbreviations

CYP	cytochrome P450 epoxygenase
EET	epoxyeicosatrienoic acid
AA	arachidonic acid
COX	cyclooxygenase
LOX	lipoxygenase
MCAO	middle cerebral artery occlusion

References

Alkayed NJ, Narayanan J, Gebremedhin D, Medhora M, Roman RJ, Harder DR. Molecular characterization of an arachidonic acid epoxygenase in rat brain astrocytes. Stroke. 1996; 27(5): 971–979. [PubMed: 8623121]

Alkayed NJ, Birks EK, Narayanan J, Petrie KA, Kohler-Cabot AE, Harder DR. Role of P-450 arachidonic acid epoxygenase in the response of cerebral blood flow to glutamate in rats. Stroke. 1997; 28(5):1066–1072. [PubMed: 9158651]

Alkayed NJ, Goyagi T, Joh HD, Klaus J, Harder DR, Traystman RJ, Hurn PD. Neuroprotection and P450 2C11 upregulation after experimental transient ischemic attack. Stroke. 2002; 33(6):1677–1684. [PubMed: 12053011]

An L, Qin J, Wang RK. Ultrahigh sensitive optical microangiography for in vivo imaging of microcirculations within human skin tissue beds. Optics Express. 2010; 18(8):8220–8228. [PubMed: 20588668]

Athirakul K, Bradbury JA, Graves JP, DeGraff LM, Ma J, Zhao Y, Couse JF, Quigley R, Harder DR, Zhao X, Imig JD, Pedersen TL, Newman JW, Hammock BD, Conley AJ, Korach KS, Coffman TM, Zeldin DC. Increased blood pressure in mice lacking cytochrome P450 2J5. FASEB J. 2008

Bylund J, Kunz T, Valmsen K, Oliw EH. Cytochromes P450 with bisallylic hydroxylation activity on arachidonic and linoleic acids studied with human recombinant enzymes and with human and rat liver microsomes. J Pharmacol Exp Ther. 1998; 284(1):51–60. [PubMed: 9435160]

Chen W, Yang S, Ping W, Fu X, Xu Q, Wang J. CYP2J2 and EETs protect against lung ischemia/ reperfusion injury via anti-inflammatory effects in vivo and in vitro. Cell Physiol Biochem. 2015; 35(5):2043–54. [PubMed: 25870948]

Daikh BE, Lasker JM, Raucy JL, Koop DR. Regio- and stereoselective epoxidation of arachidonic acid by human cytochromes P450 2C8 and 2C9. J.Pharmacol.Exp.Ther. 1994; 271(3):1427–1433. [PubMed: 7996455]

Davis CM, Siler DA, Alkayed NJ. Endothelium-derived hyperpolarizing factor in the brain: influence of sex, vessel size and disease state. Womens Health (Lond Engl). 2011; 7(3):293–303. [PubMed: 21612351]

Edin ML, Wang Z, Bradbury JA, Graves JP, Lih FB, DeGraff LM, Foley JF, Torphy R, Ronnekleiv OK, Tomer KB, Lee CR, Zeldin DC. Endothelial expression of human cytochrome P450 epoxygenase CYP2C8 increases susceptibility to ischemia-reperfusion injury in isolated mouse heart. FASEB J. 2011; 25(10):3436–47. [PubMed: 21697548]

Enayetallah AE, French RA, Thibodeau MS, Grant DF. Distribution of soluble epoxide hydrolase and of cytochrome P450 2C8, 2C9, and 2J2 in human tissues. J Histochem Cytochem. 2004; 52:447–54. [PubMed: 15033996]

Feng W, Xu X, Zhao G, Li G, Liu T, Zhao J, Dong R, Wang DW, Tu L. EETs and CYP2J2 inhibit TNF-α-induced apoptosis in pulmonary artery endothelial cells and TGF-β1-induced migration in pulmonary artery smooth muscle cells. Int J Mol Med. 2013; 32(3):685–93. [PubMed: 23835530]

Fisslthaler B, Popp R, Kiss L, Potente M, Harder DR, Fleming I, Busse R. Cytochrome P450 2C is an EDHF synthase in coronary arteries. Nature. 1999; 401(6752):493–497. [PubMed: 10519554]

Fulton D, McGiff JC, Quilley J. Contribution of NO and cytochrome P450 to the vasodilator effect of bradykinin in the rat kidney. Br.J.Pharmacol. 1992; 107(3):722–725. [PubMed: 1472970]

Goetz RM, Morano I, Calovini T, Studer R, Holtz J. Increased expression of endothelial constitutive nitric oxide synthase in rat aorta during pregnancy. Biochem.Biophys.Res.Commun. 1994; 205(1): 905–910. [PubMed: 7528018]

Golding EM, Kepler TE. Role of estrogen in modulating EDHF-mediated dilations in the female rat middle cerebral artery. Am.J.Physiol.Heart Circ.Physiol. 2001; 280(6):H2417–23. [PubMed: 11356593]

Harder DR, Alkayed NJ, Lange AR, Gebremedhin D, Roman RJ. Functional hyperemia in the brain: hypothesis for astrocyte-derived vasodilator metabolites. Stroke. 1998; 29(1):229–234. [PubMed: 9445355]

Huang A, Sun D, Koller A, Kaley G. Gender difference in myogenic tone of rat arterioles is due to estrogen-induced, enhanced release of NO. Am.J.Physiol. 1997; 272(4 Pt 2):H1804–9. [PubMed: 9139966]

Huang A, Sun D, Koller A, Kaley G. Gender difference in flow-induced dilation and regulation of shear stress: role of estrogen and nitric oxide. Am.J.Physiol. 1998; 275(5 Pt 2):R1571–7. [PubMed: 9791075]

Huang A, Sun D, Smith CJ, Connetta JA, Shesely EG, Koller A, Kaley G. In eNOS knockout mice skeletal muscle arteriolar dilation to acetylcholine is mediated by EDHF. Am.J.Physiol.Heart Circ.Physiol. 2000; 278(3):H762–8. [PubMed: 10710344]

Huang A, Kaley G. Gender-specific regulation of cardiovascular function: estrogen as key player. Microcirculation. 2004; 11(1):9–38. [PubMed: 15280095]

Iliff JJ, Close LN, Selden NR, Alkayed NJ. A novel role for P450 eicosanoids in the neurogenic control of cerebral blood flow in the rat. Exp.Physiol. 2007; 92(4):653–658. [PubMed: 17639071]

Koerner IP, Jacks R, DeBarber AE, Koop D, Mao P, Grant DF, Alkayed NJ. Polymorphisms in the human soluble epoxide hydrolase gene EPHX2 linked to neuronal survival after ischemic injury. J.Neurosci. 2007; 27(17):4642–4649. [PubMed: 17460077]

Koerner IP, Zhang W, Cheng J, Parker S, Hurn PD, Alkayed NJ. Soluble epoxide hydrolase: regulation by estrogen and role in the inflammatory response to cerebral ischemia. Front.Biosci. 2008; 13:2833–2841. [PubMed: 17981757]

Larsen BT, Miura H, Hatoum OA, Campbell WB, Hammock BD, Zeldin DC, Falck JR, Gutterman DD. Epoxyeicosatrienoic and dihydroxyeicosatrienoic acids dilate human coronary arterioles via BK(Ca) channels: implications for soluble epoxide hydrolase inhibition. Am J Physiol Heart Circ Physiol. 2006; 290:H491–9. [PubMed: 16258029]

Lee CR, Imig JD, Edin ML, Foley J, DeGraff LM, Bradbury JA, Graves JP, Lih FB, Clark J, Myers P, Perrow AL, Lepp AN, Kannon MA, Ronnekleiv OK, Alkayed NJ, Falck JR, Tomer KB, Zeldin DC. Endothelial expression of human cytochrome P450 epoxygenases lowers blood pressure and attenuates hypertension-induced renal injury in mice. FASEB J. 2010; 24:3770–81. [PubMed: 20495177]

Liu M, Hurn PD, Alkayed NJ. Cytochrome P450 in neurological disease. Curr.Drug Metab. 2004; 5(3):225–234. [PubMed: 15180492]

Liu W, Wang B, Ding H, Wang DW, Zeng H. A potential therapeutic effect of CYP2C8 overexpression on anti-TNF-α activity. Int J Mol Med. 2014; 34(3):725–32. [PubMed: 25017038]

Livak KJ, Schmittgen TD. Analysis of relative gene expression data using real-time quantitative PCR and the 2(-Delta Delta C(T)) Method. Methods. 2001; 25(4):402–8. [PubMed: 11846609]

Medhora M, Narayanan J, Harder D. Dual regulation of the cerebral microvasculature by epoxyeicosatrienoic acids. Trends Cardiovasc.Med. 2001; 11(1):38–42. [PubMed: 11413051]

Newman JW, Watanabe T, Hammock BD. The simultaneous quantification of cytochrome P450 dependent linoleate and arachidonate metabolites in urine by HPLC-MS/MS. J Lipid Res. 2002; 43(9):1563–78. [PubMed: 12235189]

Node K, Huo Y, Ruan X, Yang B, Spiecker M, Ley K, Zeldin DC, Liao JK. Anti-inflammatory properties of cytochrome P450 epoxygenase-derived eicosanoids. Science. 1999; 285(5431):1276–1279. [PubMed: 10455056]

Rifkind AB, Lee C, Chang TK, Waxman DJ. Arachidonic acid metabolism by human cytochrome P450s 2C8, 2C9, 2E1, and 1A2: regioselective oxygenation and evidence for a role for CYP2C enzymes in arachidonic acid epoxygenation in human liver microsomes. Arch Biochem Biophys. 1995; 320(2):380–9. [PubMed: 7625847]

Schlaeger TM, Bartunkova S, Lawitts JA, Teichmann G, Risau W, Deutsch U, Sato TN. Uniform vascular-endothelial-cell-specific gene expression in both embryonic and adult transgenic mice. Proc Natl Acad Sci U S A. 1997; 94:3058–3063. [PubMed: 9096345]

Seubert JM, Sinal CJ, Graves J, DeGraff LM, Bradbury JA, Lee CR, Goralski K, Carey MA, Luria A, Newman JW, Hammock BD, Falck JR, Roberts H, Rockman HA, Murphy E, Zeldin DC. Role of soluble epoxide hydrolase in postischemic recovery of heart contractile function. Circ. Res. 2006; 99:442–450. [PubMed: 16857962]

Shao Z, Fu Z, Stahl A, Joyal JS, Hatton C, Juan A, Hurst C, Evans L, Cui Z, Pei D, Gong Y, Xu D, Tian K, Bogardus H, Edin ML, Lih F, Sapieha P, Chen J, Panigrahy D, Hellstrom A, Zeldin DC, Smith LE. Cytochrome P450 2C8 ω3-long-chain polyunsaturated fatty acid metabolites increase mouse retinal pathologic neovascularization--brief report. Arterioscler Thromb Vasc Biol. 2014; 34(3):581–6. [PubMed: 24458713]

Spector AA, Norris AW. Action of epoxyeicosatrienoic acids on cellular function. Am.J.Physiol.Cell.Physiol. 2007; 292(3):C996–1012. [PubMed: 16987999]

Wang RK, Jacques SL, Ma Z, Hurst S, Hanson SR, Gruber A. Three dimensional optical angiography. Opt Express. 2007; 15(7):4083–4097. [PubMed: 19532651]

Wu S, Moomaw CR, Tomer KB, Falck JR, Zeldin DC. Molecular cloning and expression of CYP2J2, a human cytochrome P450 arachidonic acid epoxygenase highly expressed in heart. J.Biol.Chem. 1996; 271(7):3460–3468. [PubMed: 8631948]

Zeldin DC, DuBois RN, Falck JR, Capdevila JH. Molecular cloning, expression and characterization of an endogenous human cytochrome P450 arachidonic acid epoxygenase isoform. Arch Biochem Biophys. 1995; 322:76–86. [PubMed: 7574697]

Zeldin DC. Epoxygenase pathways of arachidonic acid metabolism. J.Biol.Chem. 2001; 276(39):36059–36062. [PubMed: 11451964]

Zhang W, Koerner IP, Noppens R, Grafe M, Tsai HJ, Morisseau C, Luria A, Hammock BD, Falck JR, Alkayed NJ. Soluble epoxide hydrolase: a novel therapeutic target in stroke. J.Cereb.Blood Flow Metab. 2007; 27(12):1931–1940. [PubMed: 17440491]

Zhang W, Otsuka T, Sugo N, Ardeshiri A, Alhadid YK, Iliff JJ, DeBarber AE, Koop DR, Alkayed NJ. Soluble epoxide hydrolase gene deletion is protective against experimental cerebral ischemia. Stroke. 2008; 39(7):2073–2078. [PubMed: 18369166]

Zhang W, Iliff JJ, Campbell CJ, Wang RK, Hurn PD, Alkayed NJ. Role of soluble epoxide hydrolase in the sex-specific vascular response to cerebral ischemia. J Cereb Blood Flow Metab. 2009; 29(8): 1475–81. 2009. [PubMed: 19471280]

Zhang G, Panigrahy D, Hwang SH, Yang J, Mahakian LM, Wettersten HI, Liu JY, Wang Y, Ingham ES, Tam S, Kieran MW, Weiss RH, Ferrara KW, Hammock BD. Dual inhibition of cyclooxygenase-2 and soluble epoxide hydrolase synergistically suppresses primary tumor growth and metastasis. Proc Natl Acad Sci U S A. 2014; 111(30):11127–32. [PubMed: 25024195]

Highlights

- Transgenic endothelial CYP2J2/ CYP2C8 expression reduces MCAO infarct in male mice, and to a lesser extent in female mice.

- Endothelial CYP2J2, but not CYP2C8, increases collateral blood flow in male mice.

- Endothelial CYP2J2/ CYP2C8 reduces post-ischemic inflammatory response in male mice.

- Endothelial CYP epoxygenase is a potential therapeutic target in male stroke patients.
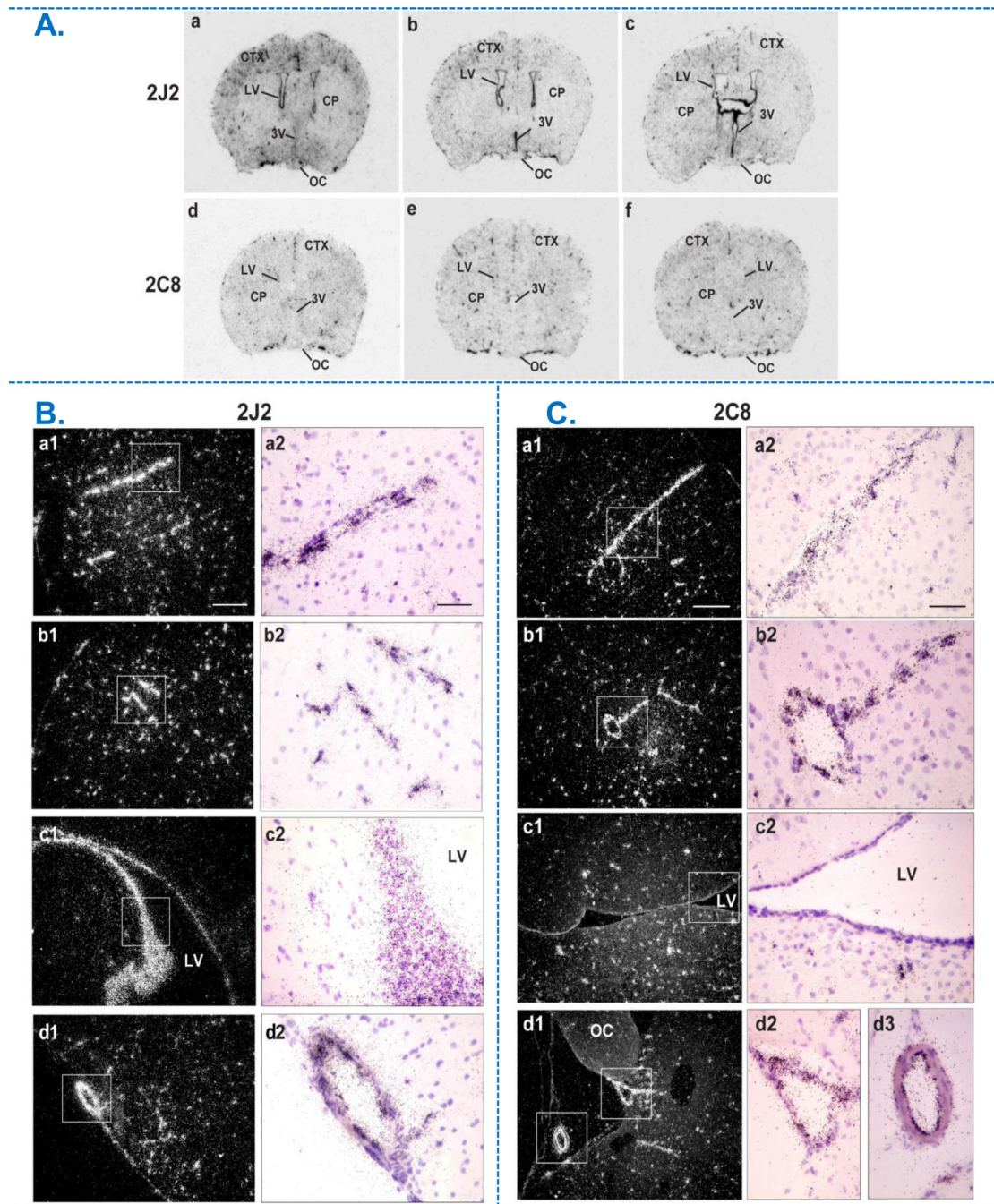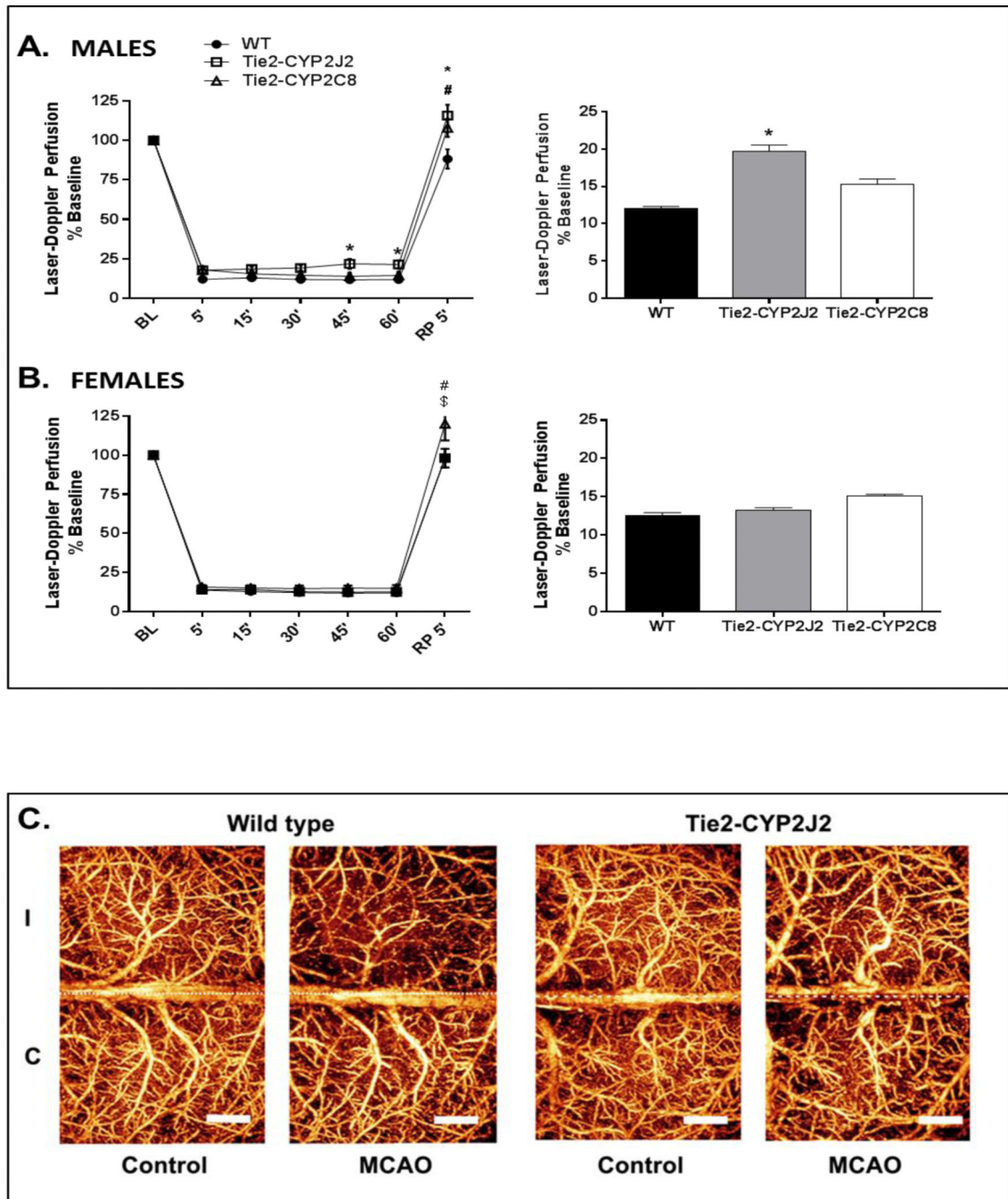
Figure 1.
Expression and distribution of human CYP2J2 and CYP2C8 mRNA in the brain of transgenic female mice by in situ hybridization (ISH). **A**. Bright-field film images illustrating the distribution of CYP2J2 (top) and CYP2C8 (bottom) mRNA (dark stain) from rostral to caudal in mouse forebrain transfected the respective human transcripts (a-c; d-f). **B & C**. Emulsion autoradiograms of human CYP2J2 (**B**) and CYP2C8 (**C**) mRNA in Tie2-CYP2J2 and Tie2-CYP2C8 mouse forebrain respectively. Photomicrographs of dark-field (a1-d1) and bright-field (a2-d2) at low and high power views, illustrating respective mRNA

signal (white grains in a1-d1, dark grains in a2-d2) within coronal sections through the rostrodorsal cortex (CTX; a, b), lateral ventricular area (LV; c) and olfactory cortex in Tie2-CYP2J2 or supraoptic nucleus area in Tie2-CYP2C8 brains (OC; d). Boxed areas from a1-d1 are shown as high-power bright-field images in a2-d2, illustrating autoradiographic grains (mRNA) over blood vessels (a,b), ependymal lining of the lateral ventricle (c) and along the ventral surface of the brain (d). Scale bar = 200 μm (a1-d1) and 50 μm (a2-d2). CP, caudate putamen; CTX, cortex; LV, lateral ventricle; OC, optic chiasm; 3V, third ventricle.

A
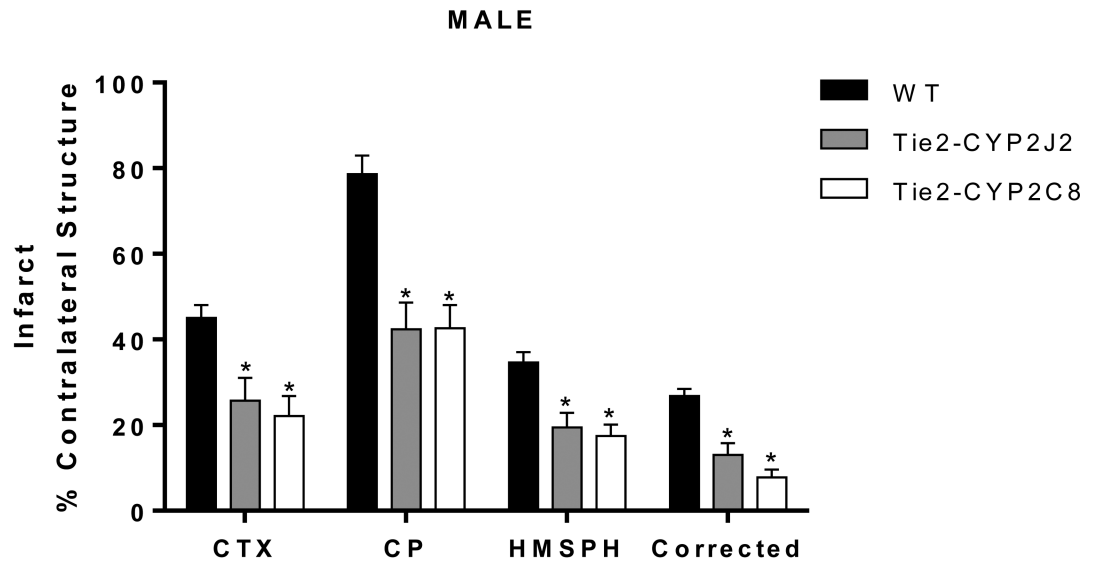
B
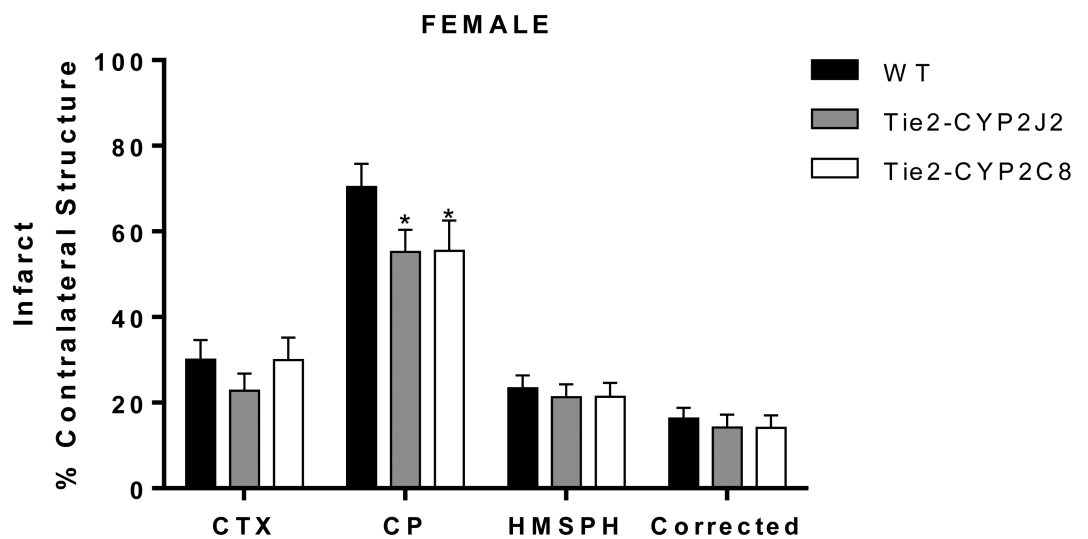
Figure 2.
Transgenic expression of CYP2J2 and CYP2C8 epoxygenase in endothelium is protective against ischemic brain injury in male (**A**) and female (**B**) mice. Infarction was assessed 24 hours after MCAO by TTC in cortex (CTX) and caudate-putamen (CP). Total hemispheric infarct is also presented as a direct measure (HMSPH) and after correcting for edema (Corrected). * p<0.05 versus WT (n=10 per group).

Figure 3.
Laser-Doppler cerebrocortical perfusion (LDP) during MCAO in WT, Tie2-CYP2J2 and Tie2-CYP2C8 male and female mice. **A**. Tie2-CYP2J2, but not Tie-2-CYP2C8 males, displayed significantly higher perfusion of the MCA territory during occlusion compared to corresponding WT males. Both Tie2-CYP2J2 and Tie2-CYP2C8 displayed higher LDP compared to WT following 5 minutes of reperfusion. **B**. No differences were observed in perfusion between female transgenic and WT mice during occlusion (n=10 per group). After 5 minutes of reperfusion Tie2CYP2C8 mice displayed higher LDP compared to both WT

and Tie2-CYP2J2 mice. Line graph displays perfusion at 15 minute intervals during occlusion and immediately following reperfusion (RP) relative to baseline (BL). Bar graph displays average perfusion throughout the occlusion period. * and # denote p<0.05 CYP2J2 and CYP2C8, respectively, versus WT; $ denotes p<0.05 Tie2-CYP2J2 versus Tie2-CYP2C8 (n=10 per group). **C.** Optical microangiography (OMAG) images illustrating increased microvascular cortical perfusion of ipsilateral ischemic (I) hemisphere in male Tie2-CYP2J2 brain 24 hours after MCAO compared to WT.
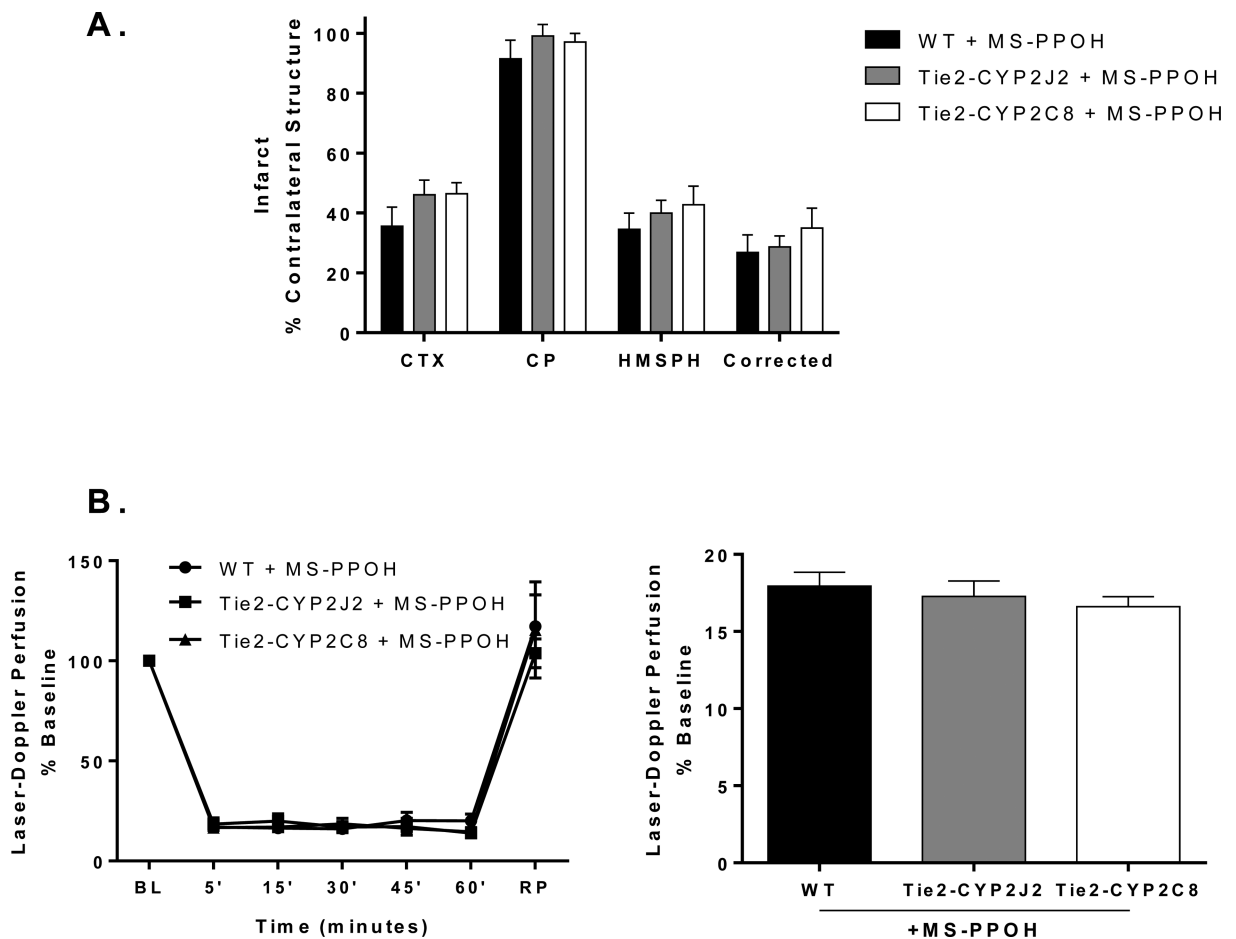
Figure 4.
Cytochrome P450 epoxygenase (CYP) inhibition abolishes protection in Tie2-CYP2J2 and Tie2-CYP2C8 male mice. **A.** Infarct size at 24 hours after MCAO was no different in transgenic compared to WT male mice in cortex (CTX), caudate- putamen (CP) or total hemisphere with (Corrected) or without correction for edema (HMSPH). **B.** Laser Doppler perfusion, at 15 minute intervals during and immediately after occlusion (left), or averaged over the occlusion period (right), was not different in male transgenic compared to WT male mice in the presence of CYP inhibitor MS-PPOH. p>0.05 (n = 5 per group).
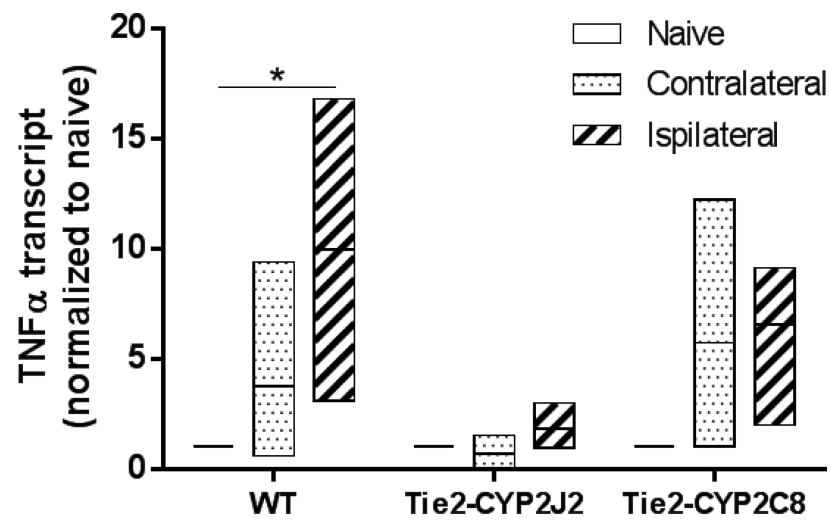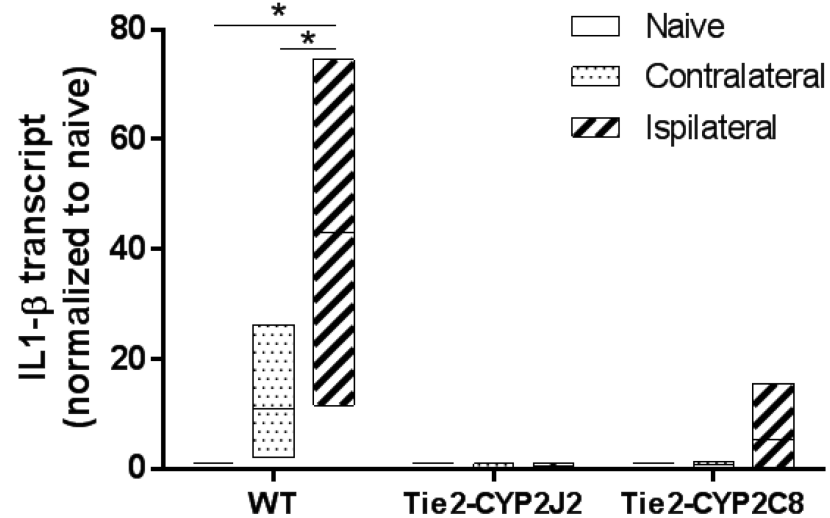
Figure 5.
Transgenic endothelial expression of CYP2J2 and CYP2C8 epoxygenase prevents ischemia-induced cytokine expression after MCAO in male mice. Levels of TNFα (**A**) and IL1-β (**B**) transcripts were assessed by qPCR in microvessels isolated from WT, Tie2-CYP2J2 and Tie2-CYP2C8 brains, at 24 hours after MCAO (both ipsilateral and contralateral hemispheres) or from naïve mice (whole brain). In WT mice, a significant increase in both TNFα and IL1-β mRNA was observed in microvessels from the ipsilateral hemisphere compared to naïve mice. No such increase was observed in microvessels from either Tie2-

CYP2J2 or Tie2-CYP2C8 transgenic mice. * $p < 0.05$ versus naive (6-9 animals per group; vessels from 3 animals were combined in one pooled sample, and 2-3 independent pooled samples were analyzed in each group).
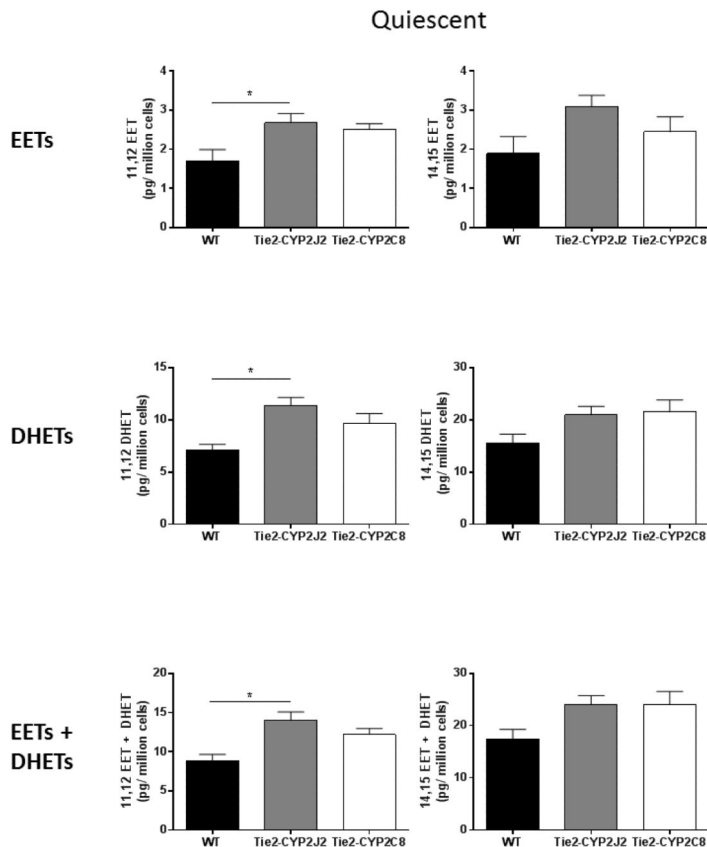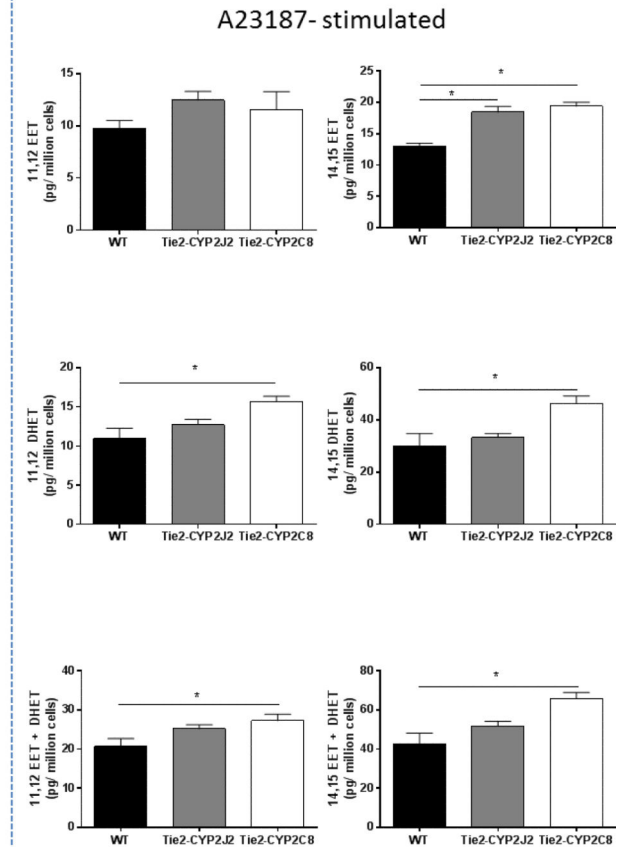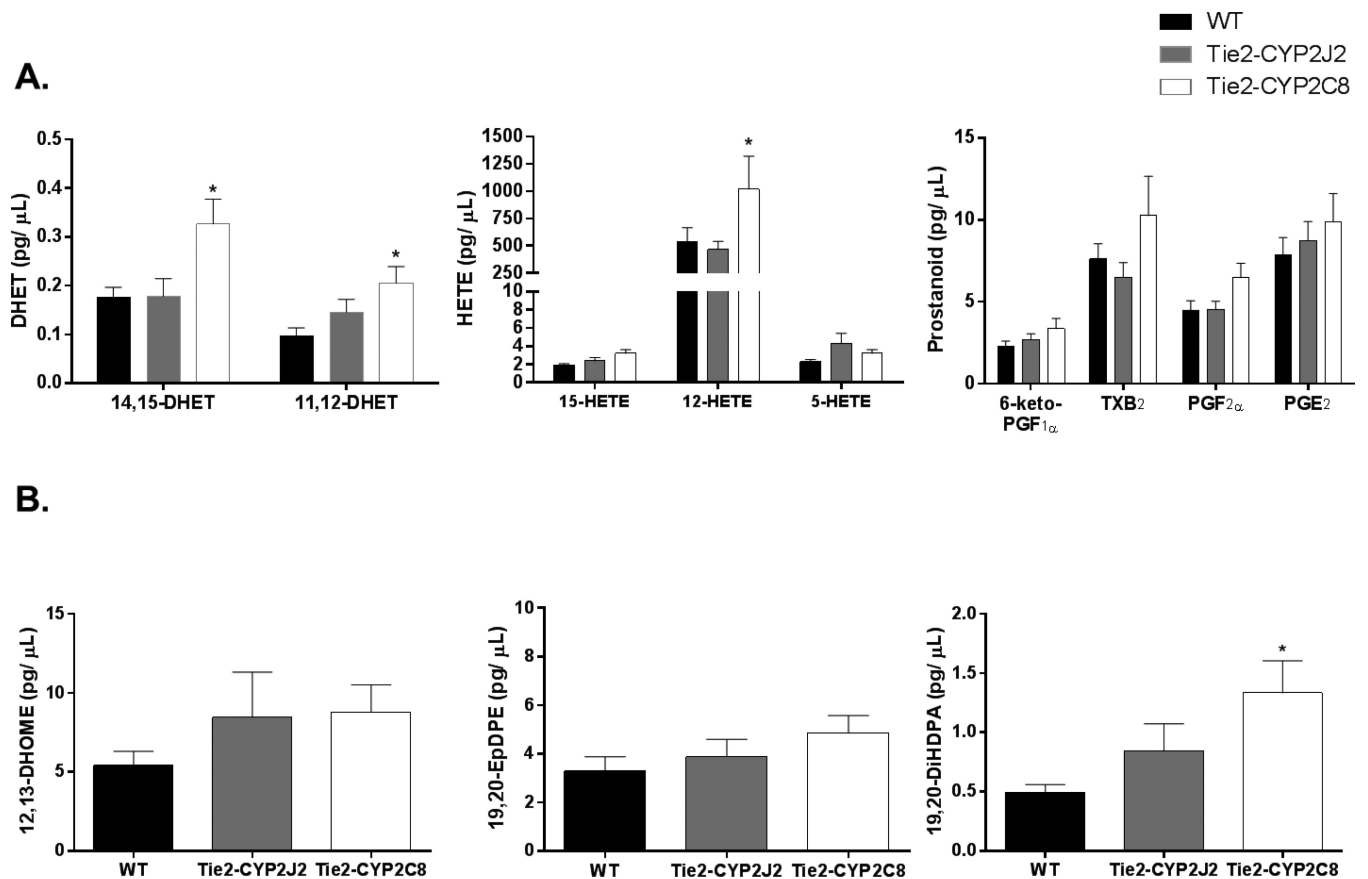
Figure 6.
Increased release of EETs and DHETs by endothelial cells from male Tie2-CYP2J2 and Tie2-CYP2C8 mice. **A**. Levels of 11,12-EET, 11,12-DHET and 11,12-EET + DHET are increased in medium conditioned by aortic endothelial cells isolated from Tie2-CYP2J2 compared to WT mice. No increase is observed in the 14,15- regioisomers or in medium collected from cells conditioned by Tie2-CYP2C8 cells. **B.** Upon stimulation of endothelial cells with A23187 calcium ionophore, cells isolated from both Tie2-CYP2J2 and Tie2-CYP2C8 mice release increased levels of 14,15-EET compared to WT cells. CYP2C8 endothelial cells also display increased DHET and EET + DHET levels of both 11,12- and 14,15- regioisomers in cell- conditioned medium, compared to WT cells.

Figure 7.
Fatty acid metabolites in CSF from male WT, Tie2-CYP2J2 and Tie2-CYP2C8 mice. **A**. Metabolites of arachidonic acid (AA) by CYP and LOX, but not COX enzymes were increased in Tie2-CYP2C8, but not Tie2-CYP2J2 mice, compared to WT. **B**. 12,13-DiHOME, a product of linoleic acid metabolism by CYP and sEH, was not different among groups. The CYP product of DHA metabolism, 19,20-EpDPE, was unaltered in CSF; however, its sEH metabolite 19,20-DiHDPA was increased in CSF from Tie2-CYP2C8 compared to WT mice. * p<0.05 versus WT (n=16 WT, 15 Tie2-CYP2J2, 11 Tie2-CYP2C8).